Incorporation of steep mountains into numerical forecasting models

By JOSEF EGGER, *Institut für theoretische Meteorologie der Universität München, Germany*

(Manuscript received December 10, 1971)

ABSTRACT

Numerical forecasting and general circulation models which include orographic effects use a smoothed topography, where the steepness of the mountains is greatly reduced. An incorporation of more realistic profiles seems desirable. To that effect a new condition at the lower boundary of the atmosphere is tested which treats steep mountains as impenetrable vertical barriers. Numerical experiments are carried out in a channel where this blocking condition is applied to an alpine profile as an example of subgrid orography and to the massiv of Greenland. Two forecasts are made for each mountain starting from an initial state which imitates a low approaching the mountain from the west in a baroclinic zonal current. The first one uses a smoothed topography and the second one applies the blocking condition to the obstacle. The latter yields patterns which agree well with synoptic experience. Cyclogenesis is predicted in northern Italy which is observed to occur typically with cold outbreaks from the north in the rear of a low. Just so, cyclogenesis is frequent near the southern tip of Greenland when a low crosses the ice cap and is predicted indeed. Both phenomena are not forecast in the experiments with smoothed topography. These and other results indicate that steep mountains are incorporated more realistically into numerical models by he new blocking condition than by a smoothed topography.

1. Introduction

Many synoptic (Walden, 1959 e.g.) and numerical (Kasahara & Washington, 1971 e.g.) studies make it clear that mountain barriers have important effects on the movement and development of cyclones and anticyclones as well as on the patterns of the general circulation. Accordingly most of the operational forecasting models and general circulation models incorporate effects of topographic features.

The way to deal with orography depends on the model's vertical coordinate. Models, which use the σ-system (Smagorinsky et al., 1965 e.g.), in which the earth's surface is always a coordinate surface, do not have a special condition for the lower boundary in the mountainous region. In models which use the z-system (Kasahara & Washington, 1971 e.g.) a kinematic condition requires at the lower boundary

$$w = \mathbf{v}_s \nabla h \quad (1)$$

where w is the vertical velocity, $\mathbf{v}_s$ is the surface wind, and h the height of the mountain. A similar condition is applied if the pressure p is chosen as a vertical coordinate (Benwell et al., 1971). All these models use a smoothed topography mostly based on the topographic charts prepared by Berkofsky & Bertoni (1955), who averaged the heights from the World Aeronautic Charts by eye over one-degree squares and averaged these values again over five-degree squares to obtain the final topography. If this smoothing increment is too large compared to the breadth of an orographic barrier, then the effective barrier height and the slopes will overly be reduced. A high knife edge mountain would be smoothed to zero by such a procedure when in fact it would have stopped all air from flowing normal to it. On the other hand, a scale analysis following Burger (1958) reveals that the slope of the mountains in a hydrostatic model should be of the order of $(f|\mathbf{v}_s|/0.1\ g) \sim 1$–

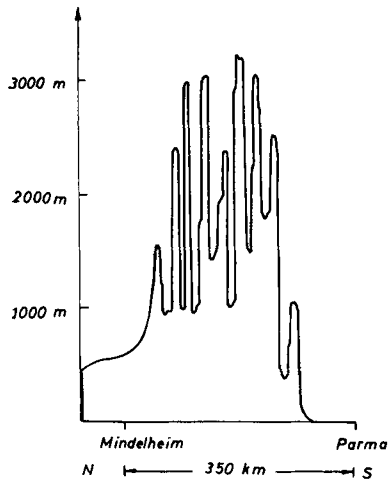

Fig. 1. North-south cross-section of the Alps along the line Mindelheim–Parma.

$2\ 10^{-3}$. An investigation of the smoothed topography of Berkofsky & Bertoni (1955) shows that the upper limit of the slopes is 10^{-2}. It is, therefore, not possible to use topographic charts which exhibit more realistic slopes than those tabulated in Berkofsky's (1955) paper. Such smooth slopes, however, are found in the interior of Greenland or in the Antarctic but normally the mountains rise to considerable heights within the range of several kilometers. Fig. 1 shows a cross-section of the alpine profile along the line Mindelheim-Parma. The vertical scale has been chosen according to the model which will be used in this paper, i.e. the thickness of the lowest layer of the model of about 2 000 m equals the horizontal distance $d = 350$ km of two adjacent grid points. The mountains look like barriers and not like hills with gentle slopes. Therefore one should try to treat them as such in numerical models.

Many models contain impenetrable vertical walls at their lateral boundaries (Smagorinsky et al., 1965 e.g.). The boundary condition is

$$v_n = 0 \qquad (2)$$

where v_n is the component of the wind normal to the wall. Accordingly one should use the condition (2) on the border of steep mountain barriers in the lower layers of the numerical models. It is the purpose of this paper to study the effect of such a blocking for various mountain profiles.

2. Model description

The way to deal with the blocking effect of mountains depends on the model which is used. The results which will be presented in this paper have been obtained by experiments with a σ-model which is very similar to that described by Edelmann (1963). This model is based on the primitive equations. A staggered grid is used for the numerical integration. It has a mesh width of 350 km and five layers in the vertical. The vertical structure of the model is presented in Fig. 2.

A comparison of the effects of (1) and (2) on the atmospheric flow in the model could be achieved by computing two different hemispheric forecasts starting from a real atmospheric situation. The first one should use a smoothed topography as usual and the second one should incorporate steep mountains by applying (2). The skill of both forecasts could be judged by comparison with the atmopheric development. However, lack of computer facilities made such an undertaking prohibitive. Instead, a channel has been chosen as integration domain. At both the northern and southern boundary of the channel we pose the condition: $v = 0$. The flow is assumed to be periodic in the x-direction. The β-plane approximation is applied.

The effect of the condition (2) is studied for two mountain profiles.

The orographic complex of the Pyrenees and the Alps has been chosen as an example of subgrid orography and Greenland as a mountain barrier which is large enough to be represented fairly realistically in the charts of Berkofsky & Bertoni (1955). The mountains are placed in the channel. The initial 'weather' is the same for all numerical experiments. A low approaches the mountain drifting in a baroclinic westerly current. One forecast is made by ap-

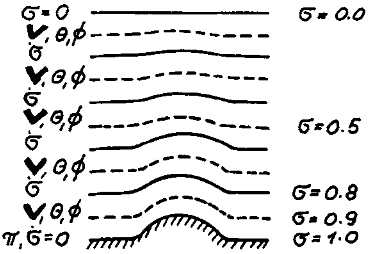

Fig. 2. Vertical structure of the model.

plying (2) to the slopes of Greenland or to the Alps and another one by using a smoothed topography. Unfortunately these forecasts cannot be evaluated by a scoring rule which relates the forecasts to the real outcome, for the forecasts start from an artificial initial situation. However much work has been devoted to studies of the behaviour of lows near Greenland and near the Alps. Walden (1959) e.g. examined the tracks of lows moving towards Greenland from the west and described the patterns which are likely to be observed. Comparing our forecasts with these results in the Greenland area it can be stated which one of the two forecasts compares more favorably with the synoptic experience. If the application of (2) yields superior results for several cases the next step should be to test this new blocking condition with an operational numerical prediction model. But, as already mentioned, such experiments have not been carried out.

3. Alps and Pyrenees

Mountain barriers like the Alps or the Pyrenees are neglected in models with grid sizes of 300–400 km for they are too small to allow a representation of their profile in the grid. A mountain should have at least a diameter of two grid sizes for any direction (Egger, 1971*b*). This condition is not satisfied by the Alps nor by the Pyrenees. Therefore the coordinate surface $\sigma = 1$ has to coincide with the flat earth in our model. On the other hand it is obvious that these barriers have a pronounced effect on the weather in Europe. There has been an attempt by the author (1971*a*) to incorporate such subgrid mountains into a forecasting model but his work was based on the boundary condition (1) and did not take into account the blocking by mountain barries.

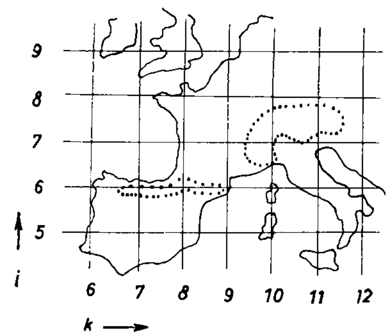

Fig. 3. Contours of the Alps, the Pyrenees and the Cantabrican mountains (dots) in the grid of the model. $k(i)$ is the index of the grid points in the $x(y)$-direction.

Fig. 3 shows the contours of the Alps, the Pyrenees and the Cantabrican mountains in the grid of the model. k (i) is the index of the grid points in the x (y)-direction. The components u, v of the wind vector are defined in the points $(k;\ i+1/2)$, $(k+1/2;\ i)$ at even time steps, resp. The situation is reversed at odd time steps.

The mountains of northern Spain act as a barriers of about 800 km length and of 100 km width to northerly or southerly flow in the lowest 2 000 m of the atmosphere. Accordingly we pose the condition

$$v = 0$$

in the points (6.5; 6), (7.5; 6) at even time steps and in the points (7; 6.5), (8; 6.5) at odd time steps in the coordinate surface $\sigma = 0.9$.

The Alps have crest heights between 3 500–4 000 m in their western part and of about 3 000 m in their eastern part. They will block any flow in the lowest 2 000 m of the atmosphere in the alpine region and most of the flow in the layer $0.8 \geq \sigma \geq 0.6$ at least in their western part. Table 1 presents the blocking conditions which have been chosen in the alpine area. These

Table 1. *Blocking conditions in the grid points of the alpine area in experiment II*

Even time steps		Odd time steps	
Grid point		Grid point	
$v = 0$	(9.5; 7); $\sigma = 0.9$ and $\sigma = 0.7$;	$v = 0$	(10; 6.5); $\sigma = 0.9$ and $\sigma = 0.7$;
	(10.5; 8); $\sigma = 0.9$ and $\sigma = 0.7$;		(10; 7.5); $\sigma = 0.9$ and $\sigma = 0.7$;
	(11.5; 8); $\sigma = 0.9$		(11; 7.5); $\sigma = 0.9$
$u = 0$	(10; 6.5); $\sigma = 0.9$ and $\sigma = 0.7$;	$u = 0$	(9.5; 7); $\sigma = 0.9$ and $\sigma = 0.7$;
	(10; 7.5); $\sigma = 0.9$ and $\sigma = 0.7$;		(10.5; 8); $\sigma = 0.9$ and $\sigma = 0.7$;
	(11; 7.5); $\sigma = 0.9$		(11.5; 8); $\sigma = 0.9$;

Table 2. *Blocking conditions in the grid points of the alpine area in experiment III*

Even time steps	Odd time steps
Grid point	Grid point
$v = 0$ (10.5; 8); $\sigma = 0.9$;	$v = 0$ (10; 7.5); $\sigma = 0.9$;
(11.5; 8); $\sigma = 0.9$;	(11; 7.5); $\sigma = 0.9$;
$u = 0$ (10; 7.5); $\sigma = 0.9$;	$u = 0$ (9.5; 7); $\sigma = 0.9$;

conditions overestimate clearly the blocking effect of the Alps. They simulate a total blocking of westerly flow over a distance of 700 km in the lowest 4 000 m of the atmosphere, whereas the Alps block westerly flow over a distance of about 450 km in the lowest 2 000 m and there is nearly nowhere total blocking in the layer $0.8 \geq \sigma \geq 0.6$. Therefore, a further experiment will be carried out using the conditions of Table 2 which underestimate somewhat the alpine blocking.

Three experiments have been performed. The initial situation is the same for all three forecasts. We have a pure zonal basic flow in the channal whose wind velocity u is a linear function of σ:

$$u = A(1 - \sigma); \quad A = 40 \text{ m sec}^{-1}.$$

The surface pressure amounts to 1 013 mb. A 20 mb low L with a diameter of about 2 000 km is superposed to this basic state. The position of the center of the low at the beginning of the forecast is marked by a cross in Figs. 4, 6, 7 west of England. The wind field of L is calculated by use of the geostrophic relation. Its vorticity is the same at all five levels and the axis of L is not tilted initially.

The first experiment (I) is made without mountains, the second one (II) uses the blocking conditions of Table 1, the third one (III) those of Table 2. II and III incorporate the mountains of northern Spain, too.

Fig. 4*a* shows the 48 h forecast of surface

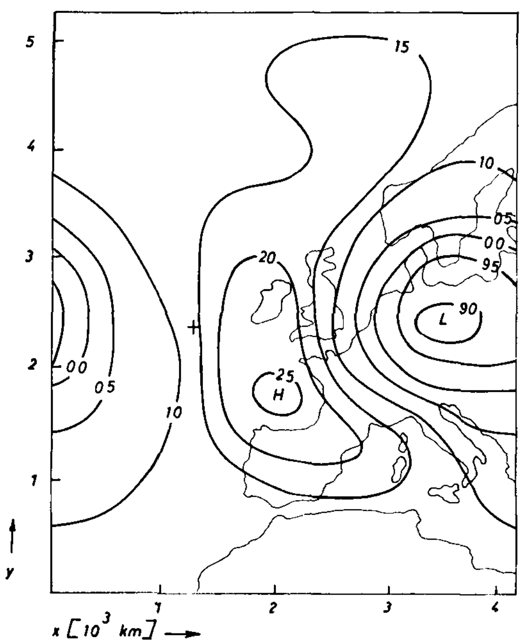

a

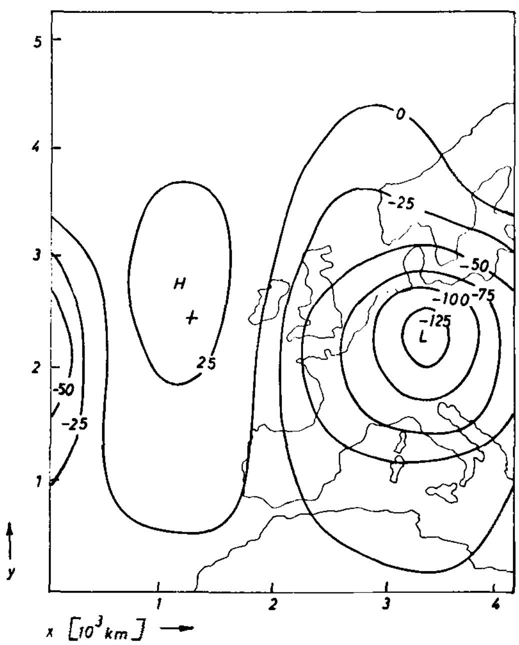

b

Fig. 4. 48 h-forecast of the surface pressure (*a*) and of the deviation of the 500 mb height (*m*) from the basic initial state (*b*) in experiment I (no mountains). The cross marks the position of the center of the low L at $t = 0h$.

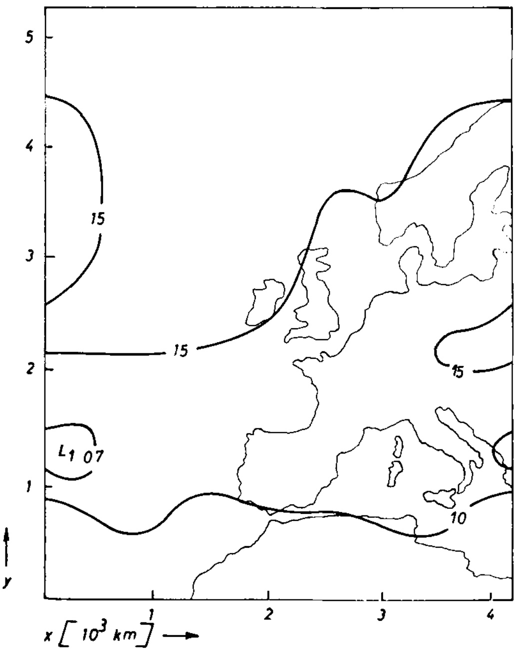

Fig. 5. 48 h-forecast of the surface pressure starting from the zonal basic state. Blocking conditions of Table 1. Exp. II*a*.

pressure for case I. The low L progressed straightforward to the east and a weak development took place. A high H developed in the rear of the low. We observe a strong pressure gradient between H and L and accordingly we have northerly flow of cold air over England, France and Italy. The deviation of the 500 mb height from the zonal basic state after 48 h can be seen in Fig. 4*b*. The patterns are quite similar to those of Fig. 4*a*. The center of H is displaced to the northwest compared with Fig. 4*a*.

Before studying the behaviour of L under blocking conditions a preliminary experiment II*a* has been carried out starting from the zonal basic state without the low L and applying the conditions of Table 1. After 12 h a small Low L_1 appears over northern Italy and a high is seen over the Alps. The development of both seems to be finished after 20 h. After 48 h (Fig. 5) a weak ridge extends from the Alps towards the east and L_1 has drifted with the westerly flow to the Aegean Sea and moves now towards Spain due to our periodic boundary conditions. This pattern is in good agreement with the results of numerical studies of air flow near the Alps with a fine mesh model (Egger, 1970). Looking for a confirmation of our result by synoptic experience we find a detailed analysis of cases of cyclogenesis in the lee of the Alps in a report of CENFAM (1963). If we accept the classification scheme outlined in this paper our case comes under category *A*: orographic cyclogenesis in prevailing zonal flow. The zonal flow is disturbed in the alpine region, a high is established north of the Alps and a low develops over northern Italy just as predicted in our case. In the 15 year period 1947–1961 156 cases of such a cyclogenesis have been observed. Unfortunately no statistics are available on the further path of the low.

Next, we superpose the low L to the basic flow west of England at $t = 0h$ (experiment II). Again, a low L_1 develops over northern Italy as a reaction of the zonal flow to the mountain blocking, and is drifting along towards the east. But now L_1 continues to deepen and a second depression L_2 develops in the lee of the Alps with the approach of L to the continent. After 48 h (Fig. 6*a*) both lows can be clearly distinguished in the sea level chart. L_1 with its center west of Spain might correspond to the low L_1 of the preceding experiment but it has a considerable greater intensity. The center of L_2 is still situated over Italy. The development of L_2 seems to simulate a type of cyclogenesis which happens very frequently in the lee of the Alps (type B in the report of CENFAM (1963)). It occurs typically with cold outbreaks from the north or northwest. 721 cases of such a cyclogenesis have been observed in the years 1947–61 in the surface niveau, 485 cases in 500 mb. Comparing Fig. 6*a* with Fig. 4*a* we seen that the track of L has curved towards the north and that a small ridge has developed north of the Alps due to the mountain blocking. L has been weakened. Also the 500 mb forecast differs considerably from Fig. 4*b*. Cyclogenesis has occurred even in this level and the filling of L is pronounced.

Fig. 7 shows the 48 h forecasts which are obtained by use of the blocking conditions of Table 2. The sea level pattern is very similar to that of Fig. 6*a* but the area and the intensity of the cyclonic activity in the lee of the Alps are reduced, as had to be expected. L_1 might be identified with the depression east of the Alps. Again we observe a northward curving of the

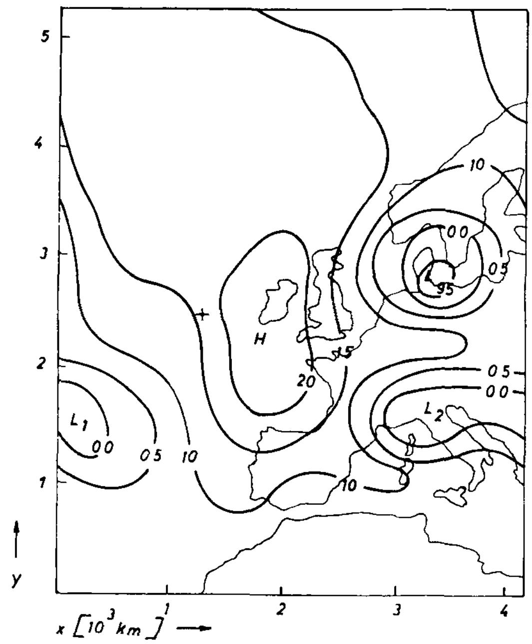

a

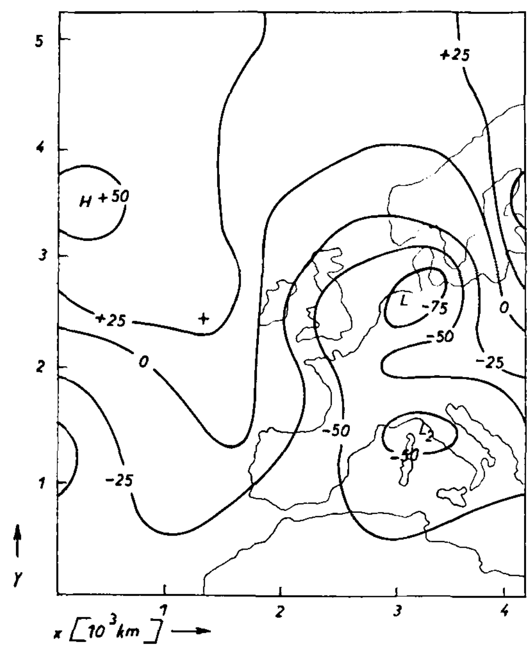

b

Fig. 6. 48 h-forecast of the surface pressure (*a*) and of the deviation of the 500 mb height (*m*) from the basic initial state (*b*) in experiment II (blocking condition of Table 1).

track of L and a ridge over the Alps. No cyclogenesis has occurred in 500 mb (Fig. 7*b*). Only a weakening of L due to orographic influences can be seen as in Fig. 6*b*.

It is not possible to decide which one of the two blocking conditions yields more realistic forecasts. But it can be presumed that an operational forecasting model, which includes orographic blocking, would have predicted most of the 877 cases of cyclogenesis in northern Italy during the 15 year period 1947–1961. On the other hand, it is sure that a model which neglects subgrid orography would have missed all cases, and perhaps it would have also missed the curving of the tracks of lows over Denmark and northern Germany, which is frequently observed (Klein, 1957).

4. Greenland

The huge massiv of Greenland, located partly in the predominant tracks of cyclones, exerts a pronounced influence on the weather in the Northern Atlantic and even in Europe (Walden, 1959). The incorporation of this island into numerical models by use of the smoothed topography of Berkofsky & Bertoni (1955) should lead to satisfying results, for Greenland is the only barrier in the Northern Hemisphere where the real barrier height (2 500–3 100 m) is closely approximated by the smoothed topography. Along the coast, however, an enormous wall rises from sea level to a height of 1 500–2 000 m blocking any flow normal to the coast line. This barrier is not represented in the smoothed topography and can only be incorporated into our model by applying (2) along the coast line. To this effect we split a somewhat idealized topography $h(x, y)$ of Greenland into two parts as shown in Fig. 8:

$$h = h_b + h_s$$

h_b represents the base of Greenland with the steep slope along the coast. It is assumed that the barriers have the same height on both sides of Greenland. Although this assumption is not quite correct it may be accepted within the limits of the coarse vertical resolution of our model. The gentle slope of the ice cap is described by ∇h_s.

Fig. 9 shows the contour of Greenland, the barrier (dots), the contours of h_s and the grid of

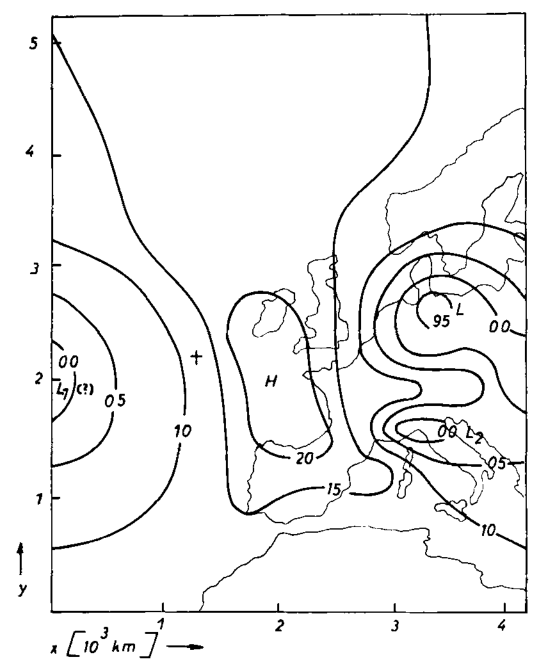

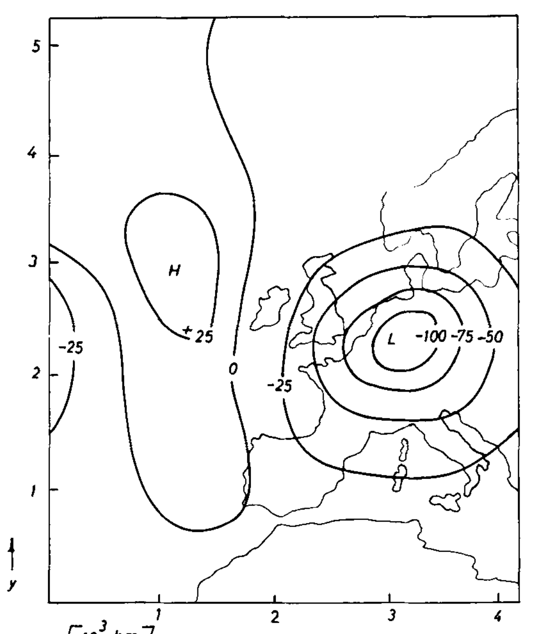

Fig. 7. 48 h-forecast of the surface pressure (*a*) and of the deviation of the 500 mb height (*m*) from the basic initial state (*b*) in experiment III (blocking conditions of Table 2).

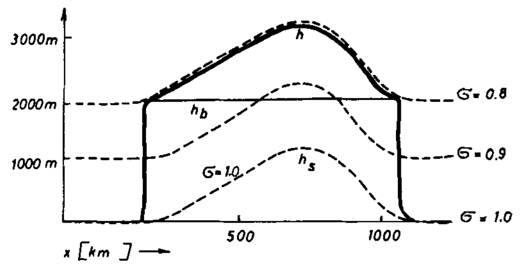

Fig. 8. West–east cross-section of Greenland and the lower levels of the model.

the model. According to Fig. 8 we have to apply the condition (2) along the barrier. Fortunately, the layer $1.0 \geqslant \sigma \geqslant 0.8$ has a thickness of about 2 000 m outside of Greenland. Therefore, if the height h_1 of the bottom $\sigma = 1$ is chosen in such a way that $h_1 = h_s$, the surface $\sigma = 0.8$ coincides with the surface of the ice cap over Greenland (see Fig. 8). Accordingly we have to pose the conditions

$$\frac{d\sigma}{dt} = 0$$

for $\sigma = 0.8$ and

$$u = v = 0$$

for $\sigma = 0.9$ in all grid points inside the barrier. The detailed modifications of the wind field

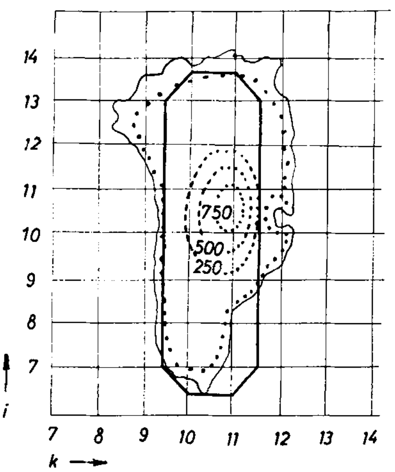

Fig. 9. Contour of Greenland, the barrier along the coast of Greenland (dots), the simulated barrier at odd time steps (solid line) and the height contours (*m*) of the reduced topography h_s in the grid of the model.

Table 3. *Blocking conditions in the Greenland area in the σ-surface σ = 0.9*

The symbol $\{u(k;i), v(j;l)\} \| \{1, -1\}$ e.g. means that at each time step of the numerical integration only that component of the computed horizontal wind vector $\{u, v\}$ is retained, which is parallel to the vector $\{1, -1\}$, where u is defined in the grid point with the indices k, i and v in the point with j, l

Even time steps	Odd time steps
$u = 0$ in the grid points:	$u = 0$ in the grid points:
$(k; i+1/2)$, $10 \leq k \leq 11$, $8 \leq i \leq 12$;	$(k+1/2; i)$, $10 \leq k \leq 11$, $8 \leq i \leq 12$;
(11; 7.5); (11; 13.5).	(10.5; 7); (10.5; 13).
$v = 0$ in the grid points:	$v = 0$ in the grid points:
$(k+1/2; i)$, $10 \leq k \leq 11$, $8 \leq i \leq 13$;	$(k; i+1/2)$, $10 \leq k \leq 11$, $7 \leq i \leq 12$
and	and
$\{u(10; 7.5), v(10.5; 7)\} \| \{1, -1\}$	$\{u(9.5; 7), v(10; 6.5)\} \| \{1, -1\}$
$\{u(12; 7.5), v(11.5; 7)\} \| \{1, 1\}$	$\{u(11.5; 7), v(11; 6.5)\} \| \{1, 1\}$
$\{u(10; 13.5), v(10.5; 14)\} \| \{1, 1\}$	$\{u(9.5; 13), v(10; 13.5)\} \| \{1, 1\}$
$\{u(12; 13.5), v(11.5; 14)\} \| \{1; -1\}$	$\{u(11.5; 13), v(11; 13.5)\} \| \{1, -1\}$

along the barrier and in the grid points of the interior of Greenland can be seen from Table 3. The corresponding simulated barrier is shown in Fig. 9 (solid line) for even time steps. It is obvious that this approximation to the real barrier is very crude but it was thought that modifications and refinements should be made after experience has been gained with a simplified contour of the barrier. The nondimensional surface pressure π and the potential temperature are calculated as usual inside and along the barrier. π describes the pressure distribution at the bottom of the model when the layer $1 \geq \sigma \geq 0.8$ of ice and rock inside the barrier is replaced by air of the calculated temperature.

Two experiments have been carried out. The first one uses a smoothed topography, the second one applies the blocking technique. The initial fields are the same as those used for the runs of chapter 3—a zonal baroclinic flow to which a low L is superposed west of Greenland. In the mountain area the surface pressure is modified in such a way that the wind field which is computed according to the geostrophic relation is the same as outside the Greenland area. Therefore, the wind is not adjusted to the slope of the mountain and even without a low L the forecasts show quite interesting patterns. Initially, the air is forced to ascend on the windward side and is pouring down the leeward side. The zonal flow is perturbed to form a ridge over Greenland and a low L_1 in the lee which is moving eastwards. This pattern is quite similar to that obtained by the simulation of the Alps in chapter 3, but the intensity of the perturbations is much greater. L_1 has now an amplitude of 12 mb and a diameter 2 000 km after 48 h in the case with smoothed topography.

Fig. 10 shows the deviations of the surface pressure and of the 500 mb height from the basic state to which the low L was superposed at $t = 0h$, after 48 h for the case with smoothed topography. The dots mark the path of the center of L. Approaching Greenland the low is retarded, curves towards the north along the west coast and is filled very rapidly (Fig. 10*a*). After 48 h a new center of low pressure is observed north of Scoresby-sund. The center on the west coast has disappeared. L_1 approaches Greenland from the west and a high has developed near the southern tip of Greenland.

Even at 500 mb (Fig. 10*b*) L is retarded when approaching Greenland. The center curves towards the south and finally the ice cap is crossed very fast.

The forecast with mountain blocking is presented in Fig. 11. The center of the surface low remains on the east coast and begins to fill after 36 h. Cyclogenesis occurs at the end of the first day near the southern tip of Greenland and a strong pressure fall is observed along the east coast. After 48 h a 25 mb low has developed in the sea level. Aloft, the center of L is forced to curve southward by a strong high northeast

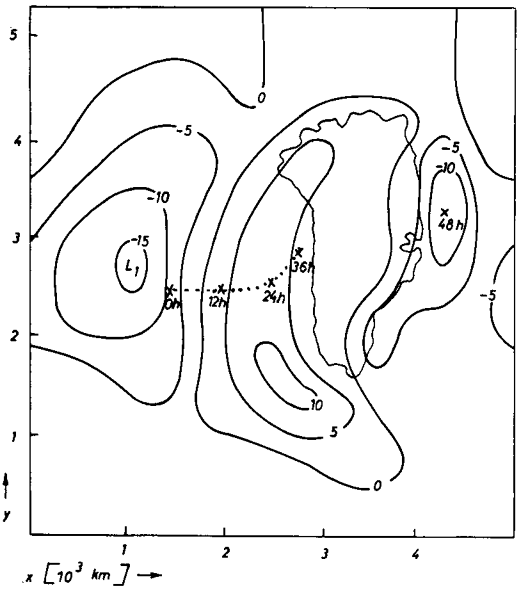

a

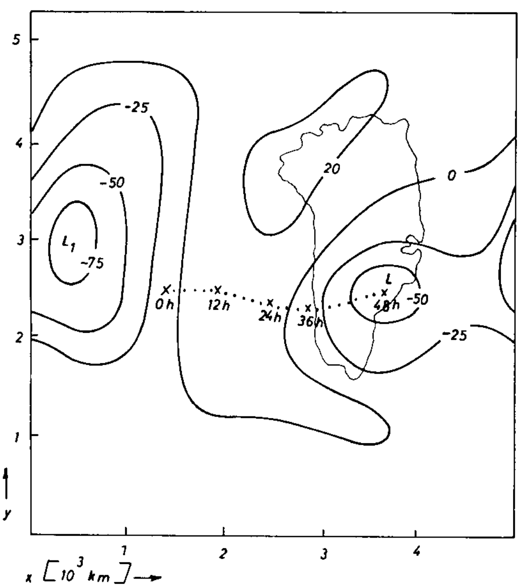

b

Fig. 10. Deviation of the surface pressure (*a*) and of the 500 mb height (*m*) (*b*) from the basic initial state after 48 h in the experiment with smoothed topography. The track of the center of *L* is marked by dots.

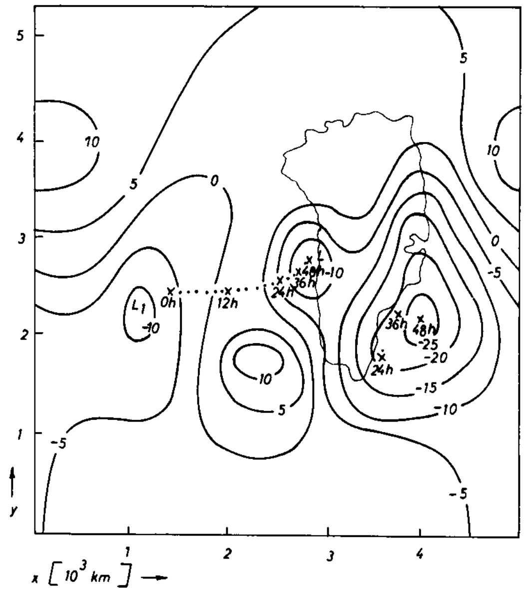

a

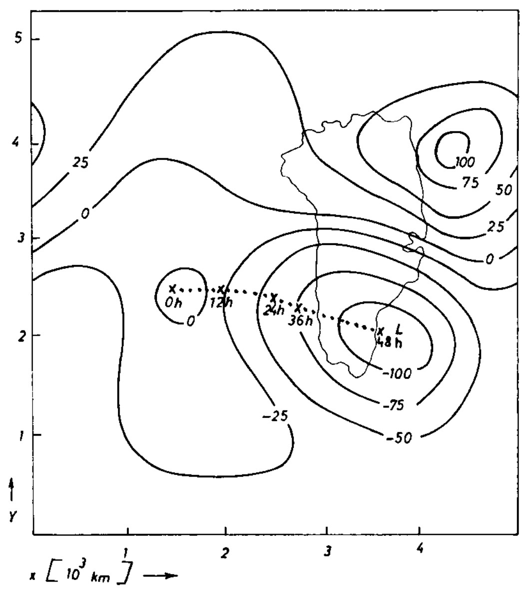

b

Fig. 11. Deviation of the surface pressure (*a*) and of the 500 mb height (*m*) (*b*) from the basic initial state after 48 h in the experiment with blocking conditions.

of Greenland. *L* is much more intense in Fig. 11*b* than in Fig. 10*b*. L_1 on the contrary, can hardly be detected in Fig. 11.

The most thorough study of the behaviour of lows near Greenland has been made by Walden (1959). He defined 52 weather patterns. However, he found that most of the types could be collected into four groups depending on the prevailing direction of the storm track. Our case comes under group A: A low moving from a direction between southwest and west-northwest towards the central part of Greenland. Twelve different types are included in this group. The types A_3, A_6, A_7 are most close to the patterns shown in Fig. 10–11. The surface center of a low which extends to great heights is retarded when approaching Greenland and curves northward along the west coast. In the mean time the pressure begins to fall on the eastern coast. A low develops near Cap Farewell (A_6, A_7) or somewhat more towards the north (A_3) before the upper trough has crossed the ice cap. These three types comprise 57 % of all cases of group A observed from January 1948 to December 1957. No case is shown where the development of the surface low on the east coast takes place north of the lows track at 500 mb as it is forecast in Fig. 10. It can be stated, therefore. that the patterns which are obtained by applying the blocking condition are more likely to be observed than those shown in Fig. 10.

5. Numerical problems

The integral of total energy for the flow in the channel which may be regarded as a measure of the numerical stability showed a variation of less than 0.15 % of its initial value in all experiments. The use of blocking conditions did never result in numerical instability. Nevertheless two numerical problems turned up in the experiments on which few remarks will be made.

(a) *Wind fields*

The field of surface pressure which is presented in Fig. 7*a* shows pronounced features of the smallest scale which can be resolved by the model. The corresponding wind fields are surprisingly smooth except for the grid points on the windward side of the Alps ($k = 8$, $k = 9$) in the lowest level ($\sigma = 0.9$). Changes of the sign of v from grid point to grid point together with great wind velocities ($v \leqslant 20$ m sec^{-1}) are observed. The wind fields are sufficiently smooth for $\sigma = 0.7$. On the other hand, the wind fields computed in experiment II are smooth in the lowest layer and show only small fluctuations for $\sigma = 0.7$ on the windward side. Such a difference is obviously created by the fact, that as for experiment III the westerly flow is blocked in one grid point, only, whereas in experiment II it is blocked in two points. Three further tests have been made to clarify this problem.

In the first experiment a pure zonal flow is blocked by the condition $u = 0$ in one grid point. In the second (third) one the condition is applied at two (three) grid points which are neighbours in the y-direction ($\sigma = 0.9$). All three tests reveal acceptable pressure fields but the wind field is considerably disturbed in front of the blocking point in the first run after 24 h, somewhat 'noisy' in the second one, and smooth in the third experiment. One may formulate the rule that a blocking barrier should have a length of two grid sizes, at least. But even if the flow is blocked in one grid point, only, the region of highly disturbed wind fields seems to be restricted to some grid points on the windward side of the obstacle. There are no restrictions on the width of the barrier. No numerical noise has been created by the blocking by the Spanish mountains, for example.

(b) *Boundary conditions at the barrier of Greenland*

The boundary conditions at the barrier of Greenland, which are defined in Table 3 are somewhat unusual. In numerical experiments with lateral walls mostly one of the three possibilities listed in the paper of Baumhefner (1971) is used. Accordingly a test has been made with the so-called free slip-boundary conditions where the tangential component of the wind and the pressure are forecast at the barrier with a reflective assumption on the normal component of the wind. But after 48 h the fields of surface pressure at even points of time had begun to differ from those at odd points of time near Greenland. Such a tendency could create serious difficulties if the forecast is extended. The phenomenon is greatly reduced when the conditions of Table 3 are applied but it does not disappear totally. As an example, the deviation of surface pressure from the initial state is shown at two following points of time after 48 h in the area of cyclonic development near the southern tip of Greenland where this tendency is particularly pronounced (Table 4). The pressure is defined in the grid points (k; i) at even time steps and in the centers of the mesh squares at odd time steps. The cyclonic development is weaker at odd time steps than at even ones near the grid points (12; 9) and (12; 10).

Table 4. *Deviations of the surface pressure (mb) from the initial state after 48 h in the grid points near the southern tip of Greenland in the experiment with blocking conditions*

The pressure is defined in the grid points $(k; i)$ at even time steps and in $(k+1/2;\ i+1/2)$ at the following time step

i ↑ / k →	10		11		12		13		14
11	4.2		5.2		−15.4		0.2		6.7
		4.2		0.2		−9.9		2.3	
10	−2.2		−2.0		−21.1		−4.2		1.1
		−6.0		−8.4		−13.1		−2.8	
9	−8.2		−12.7		−24.8		−10.9		−5.1
		−12.9		−14.7		−23.4		−10.0	
8	−13.1		−13.1		−28.5		−20.1		−10.2
		−11.9		−11.8		−22.2		−15.3	
7	−2.4		−22.2		−22.3		−18.8		−12.5
		−20.4		−22.4		−16.4		−15.2	
6	−2.1		−16.8		−14.6		−12.6		−11.3
		−6.3		−11.3		−9.5		−10.3	
5	1.5		−6.0		−6.6		−6.7		−7.9

(c) Steep slopes of coordinate surfaces

Over the steep slopes of mountains fictitious eddies appear even in the highest levels of the model due to large truncation errors in the computation of the pressure gradient force. This difficulty, which is characteristic for the σ-models, can be partly overcome by using special numerical techniques, as shown by Kurihara (1967). On the other hand, the steepness of the σ-surfaces is greatly reduced if blocking conditions are applied. The maximum height difference in a σ-surface caused by the topography of Greenland, for example, does not exceed 800 m in the experiments with blocking and amounts to 2 700 m in runs with smoothed topography. Therefore, the truncation error will be reduced by the application of the blocking condition.

6. Summary and conclusions

If condition (1) is taken as the lower boundary condition only a very smooth topography can be incorporated into numerical models. Therefore, a new boundary condition has been tested, which treats steep mountains as impenetrable vertical barriers. Numerical experiments have been carried out in a channel and the blocking condition has been applied to an alpine profile and to the massiv of Greenland. Starting from an artificial initial situation, which simulates a low approaching the mountains in a uniform baroclinic westerly current, two different forecasts have been made for each profile—the one using a smoothed topography and the other one applying the blocking condition. The latter yielded patterns which agree well with synoptic experience. Cyclogenesis in the Gulf of Genoa and over northern Italy has been predicted which occurs typically with cold outbreaks from the north in the rear of a low. Cyclogenesis near the southern tip of Greenland is common when a low crosses the ice cap and has been predicted indeed. Both phenomena have been missed by the forecasts using a smoothed topography. Therefore the experiments encourage further testing of the blocking technique in forecasts with real data.

REFERENCES

Baumhefner, D. P. 1971. On the effects of an imposed southern boundary on Numerical Weather Prediction in the northern hemisphere. *Journal of Atmospheric Science 28*, 42–54.

Benwell, G. R. et al. 1971. The Bushby-Timpson 10-level model on a fine mesh. *Met. Off., Sc. Pap. No. 32*, London.

Berkofsky, L. & Bertoni, E. A. 1955. Mean topographic charts for the entire earth. *Bull. Amer. Met. Soc. 36*, 350–354.

Burger, A. P. 1958. Scale considerations of planetary motions of the atmosphere. *Tellus 10*, 195–205.

CENFAM 1963. Research work on the project "Cyclone Development in the Lee of the Alps". S.T.R. No. 4, Rome.

Edelmann, W. 1963. On the behaviour of disturbances in a baroclinic channel. *Res. Div. German Weather Service, Tech. Note 7.*

Egger, J. 1970. On the simulation of subgrid orographic effects in numerical forecasting. *J. Atm. Sc. 27*, 896–902.

Egger, J. 1971*a*. On the treatment of subgrid orography in a baroclinic forecasting model. *J. Atmos. Sc.* 28, 1144–1152.

Egger, J. 1971*b*. Mindestgröße von Gebirgen und Konvektionsgebieten, die in den Modellen der numerischen Vorhersage berücksichtigt werden können. *Beitr. Phys. Atm.* 44, 245–271.

Kasahara, A. & Washington, W. M. 1971. General circulation experiments with a six-layer NCAR model including orography, cloudiness and surface temperature calculation. *J. Atm. Sc. 28*, 657–701.

Klein, W. 1957. Principal tracks and mean frequencies of cyclones and anticyclones in the northern hemisphere. *Res. Pap. No. 40, U.S. Dep. Com.*

Kurihara, Y. 1967. Note on finite difference expressions for the hydrostatic relation and pressure gradient force. *Month. Weath. Rev. 95.*

Putnins, P. 1970. The climate of Greenland. In *World Survey of Climatology; Climate of the Polar Regions.* Elsevier Publ. Comp., Amsterdam, London and New York.

Smagorinsky, J. et al. 1965. Prediction experiments with a general circulation model. *Proc. Symp. Dynamics Large-Scale Atm. Proc.* Moscow, 70–134.

Walden, H. 1959. Statistisch-synotische Untersuchungen über das Verhalten von Tiefdruckgebieten im Bereich von Grönland. *Deutscher Wetterdienst, Seewetteramt*, Einzelver. 20.

УЧЕТ КРУТЫХ ГОР В МОДЕЛИ ЧИСЛЕННОГО ПРОГНОЗА

Модели для прогноза и общей циркуляции, учитывающие орографические эффекты, используют сглаженную топографию, где крутизна гор сильно преуменьшена. Представляется желательным учет более реалистических профилей. Для этого испытывается новое условие на нижней границе атмосферы, которое трактует крутые горы как непроницаемые вертикальные барьеры. Проведены численные эксперименты в канале, где это условие блокировки применены к альпийскому профилю, как примеру подсеточной орографии, а также к гренландскому массиву. Для каждого горного массива выполнены два прогноза от начального состояния, имитирующего приближение с запада к горам области низкого давления в бароклинном зональном потоке. В первом прогнозе используется сглаженная топография, а во втором — применяется условие блокировки на препятствии. В последнем случае получается картина, хорошо согласующаяся с синоптическим опытом. Предсказан циклонез в Северной Италии, который обычно происходит при холодных вторжениях с севера с тыла области низкого давления. Точно также, циклонез часто наблюдается вблизи южной оконечности Гренландии, когда область низкого давления пересекает ледяной купол острова, что также предсказывается в модели. Оба явления не предсказываются в экспериментах со сглаженной топографией. Эти и другие результаты показывают, что крутые горы более реалистично учитываются в численных моделях при использовании нового условия типа блокировки, чем в случае сглаженной топографии.